Chemistry
A European
Journal

Chemistry Europe
European Chemical Societies Publishing

Accepted Article

Title: Chemotactic Colloidal Motor

Authors: Chang Zhou, Ling Yang, Yingjie Wu, Mingcheng Yang, and Qiang He

To be cited as: *Chem. Eur. J.* **2022**, e202202319

Link to VoR: https://doi.org/10.1002/chem.202202319

WILEY-VCH

10.1002/chem.202202319

WILEY-VCH

CONCEPT

Chemotactic Colloidal Motor

Chang Zhou,[a,b] Ling Yang,[b] Yingjie Wu,*[a] Mingcheng Yang,[c] and Qiang He*[a,b]

[a] C. Zhou, Dr. Y. J. Wu, Prof. Q. He
Key Laboratory of Microsystems and Microstructures Manufacturing (Ministry of Education), School of Medicine and Health
Harbin Institute of Technology, No. 92 XiDaZhi Street, Harbin, 150001, China
E-mail: wuyingjie@hit.edu.cn, qianghe@hit.edu.cn
[b] C. Zhou, Dr. L. Yang, Prof. Q. He
Wenzhou Institute, University of Chinese Academy of Sciences, 1 Jinlian Street, Wenzhou 325000, China
[c] Prof. M. C. Yang
Beijing National Laboratory for Condensed Matter Physics and Laboratory of Soft Matter Physics, Institute of Physics, Chinese Academy of Sciences, Beijing, 100190, China; School of Physical Sciences, University of Chinese Academy of Sciences, Beijing 100049, China; Songshan Lake Materials Laboratory, Dongguan, Guangdong 523808, China

Supporting information for this article is given via a link at the end of the document.

Abstract: Chemotaxis plays a crucial role in the realization of various functions of human life such as fertilization, immune function, inflammatory response, regeneration process. Inspired by the natural chemotaxis, colloidal motors with chemotactic ability can realize intelligent sense and targeted navigation, which bring a revolutionary method to biomedical applications like precision medicine. However, the application in the biomedical field requires the colloidal motors with submicrometer scale, strong chemotactic ability and clear chemotactic mechanism. In this concept article, we introduce the recent progress of chemotactic colloidal motors, covering the fundamental theory behind experimental advancements. Particularly, the torque-driven reorientation motion of the submicrometer-sized colloidal motors during chemotaxis is discussed, and also their underlying mechanism is proposed. With the continuous research on chemotactic colloidal motors, it is believed that the emerging chemotactic colloidal motors will broaden practical applications in the biomedical field.

Introduction

As a new type of active colloidal particles, the colloidal motors can convert chemical energy stored in the surrounding environment or ambient energy into their persistent swimming-like motion in fluids. Over the past decades, colloidal motors have gradually developed from a basic concept to the multi-functional micro/nanosystem with great potential in the biomedical fields. With the in-depth study of colloidal motors, it has been found that the unguided self-propelled motion of the colloidal motors can only undergo an enhanced Brownian diffusion on large timescale.[1] To realize the application of the colloidal motors in the biomedical field, precise control of their self-propelled motion is indispensable.[2] Chemotaxis is a promising way to guide the self-propelled motion of the colloidal motors.

Chemotaxis is the tendency response of organisms to the stimulation of chemical substances in the external environment, which is crucial for organisms to find food or keep away from harmful substances. Natural microorganisms such as *Escherichia coli* (*E. coli*) can sense glucose gradient and move toward the glucose-enriched area.[3] Not only in the natural microorganisms, chemotaxis is also important for the realization of various functions such as fertilization,[4] immune function,[5] inflammatory response,[6] regeneration process[7] *in vivo*. For example, leukocytes rely on chemotaxis to approach and devour foreign matter to help the body defend against infection.[8] Inspired by the chemotaxis in nature, researchers have developed chemotactic colloidal motors to realize the self-navigation toward specific region. So far, most of the chemotactic studies on the colloidal motors have been conducted *in vitro*.[9] It is widely proved that the colloidal motors can sense the gradient of the fuel in the solution and move toward the fuel-enriched area.[10] Some studies on the chemotactic colloidal motors *in vivo* indicates that the chemotaxis can guide the colloidal motors toward the diseased site by sensing the abnormal amount of substances such as H_2O_2[11] or glucose.[12] With the in-depth study on the chemotactic colloidal motors, it can be expected that the chemotactic colloidal motors can overcome the interstitial pressure compared to the passive diffusion of the drugs due to the self-propelled motion and the chemotaxis.[11b] Furthermore, combining the submicrometer size, chemotactic colloidal motors can break through the limitation of the biological barrier such as the blood-brain barrier (BBB), which can further improve the administration efficiency.[12] These advantages make the chemotactic colloidal motors high application potential in the biomedical field. However, there are also significant challenges that have prevented the *in vivo* application of the chemotactic colloidal motors.

One issue is that the chemotactic mechanism is not well understood. Some theoretical analysis and numerical simulations suggest that colloidal motors can perform chemotactic motion along the fuel gradient through aligning with the chemical gradient.[13] However, few experiments have been able to prove this hypothesis, especially for colloidal motors of submicrometer size. Furthermore, the size of the chemotactic colloidal motors has to meet the requirements for biomedical applications. Studies have found that there are various biological barriers *in vivo* such as blood-brain barrier.[14] These biological barriers can effectively prevent the body from being invaded by harmful substances, but they are also the obstacle to the active drug delivery of the chemotactic colloidal motors.[14a] To overcome those biological barriers, the colloidal motors with submicrometer-sized scale are highly requested for biomedical applications.[15] However, when the size of the colloidal motors is down to the submicrometer scale, the effect of the stochastic force from the collision of the solvent molecules is significantly increased, which drives the colloidal motors a random process and reduces the chemotactic ability. On the other hand, the submicrometer size also makes it difficult to directly observe the motion posture of the colloidal motors in the

10.1002/chem.202202319

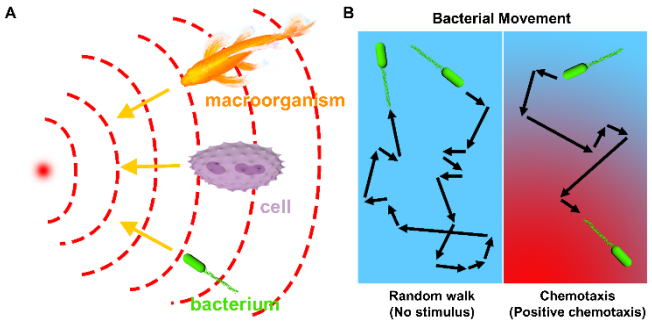

Figure 1. (A) The chemotaxis of the cells and organisms. (B) The scheme of the random walk or the positive chemotaxis of the bacteria.

chemotactic motion, which limits the detailed research on the underlying chemotactic mechanism of the submicrometer-sized colloidal motors. Hence, the submicrometer-sized colloidal motors with strong chemotactic ability can make great contribution to the biomedical applications such as the realization of active drug delivery and precision medicine.

In this concept article, we will focus on the underlying mechanism of the artificial submicrometer-sized chemotactic colloidal motors. In addition, the recent theoretical researches on the torque-driven reorientation mechanism of the submicrometer-scale colloidal motors are also discussed. We hope that the study on the chemotactic mechanism can provide new insights for the design and preparation of intelligent colloidal motors, which will contribute to the future biomedical applications.

Chemotactic Behaviors of Colloidal Motors

In nature, chemotaxis is one of the most important processes for the survival of the living organisms, which can drive them toward the chemical attractant (*e.g*. food) or away from the chemical repellents (*e.g*. toxins). The macroorganisms such as fish can sense the smell from food and achieve foraging (Figure 1A).[16] In addition, with the study on the chemotaxis of the microorganisms, it has been found that the realization of natural chemotaxis relies on the chemotactic behavior in response to chemical gradients. Consider the positive chemotaxis of *Escherichia coli* (*E. coli*), which is achieved the chemotaxis according to the run-and-tumble behavior. As shown in Figure 1B, bacteria are not able to actively reorient in a field gradient. Yet they are sensitive to the concentration of certain substances. If the *E. coli* detects a favorable change of chemical concentration along its trajectory, it turns down the tumble frequency; on the other hand, if it feels it goes the wrong direction, it augments the tumble frequency. As a consequence, the bacteria spend more time in an orientation toward the chemical attractant source.[17] However, the chemotactic motion behavior of the organisms such as the *E.coli* depends on a series of the receptors and the signaling pathways between different receptors, which makes the internal structure of the *E.coli* a complex chemotactic system. Through the cooperation of the receptors, the *E.coli* can respond to the substrate gradient and control the motion behavior of the flagella, which leads to the chemotaxis of the *E.coli*.[18] The chemotactic response system is difficult to be implemented in the artificial colloidal motors since the structure is so complex and precise that can not be prepared in this stage. In this context, the chemotaxis of the artificial colloidal motors must rely on the directional interaction between the self-propulsion and the chemical concentration gradient.[13a]

With the study on the colloidal motors, it has been found that the unguided self-propelled colloidal motors can only exhibit enhanced Brownian motion in the homogeneous solution due to the rotational diffusion.[1a] Thus, the way to guide the colloidal motors' enhanced Brownian motion is important so that the colloidal motors can realize the precise navigation. With the in-depth study on the colloidal motors, it has been developed several ways to achieve the guidance, which can be divided to the external field and the self-navigation. As for the external field, the most common way for the guidance is the magnetic field, which can precisely control the motion direction of the colloidal motors. However, the guidance of the magnetic field requires complex equipment and the magnetic nanoparticles attached to the colloidal motors. In addition, the magnetic field may influence the normal operation of the imaging system, which is an obstacle for the magnetic field applied in the biomedical field. In this case, the self-navigation is more proper for the colloidal motors to control the self-propelled direction. To realize the self-navigation, the chemotaxis is the fundament, which can make the colloidal motors sense the substrate gradient and move toward the substrate-enriched area. Compared to the external field, the chemotaxis can be achieved without other equipment and chemical modification, which is based on the couple between the chemical reaction in the colloidal motors and the substrate gradient, which makes the chemotaxis become an ideal way to realize the precise self-navigation of the self-propelled colloidal motors. To study the chemotaxis of the colloidal motors, relevant chemotactic experiments and theories are developed. Sen *et al*. prepared the Pt-Au rodlike colloidal motors (2 μm in length and

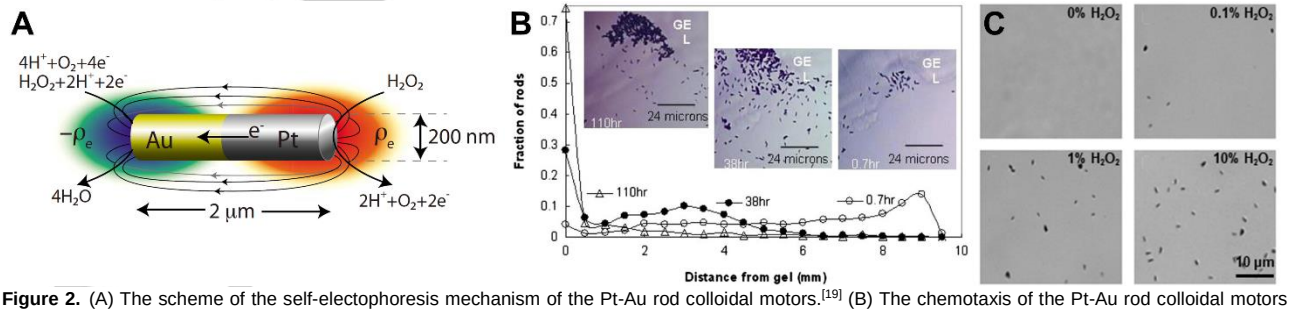

Figure 2. (A) The scheme of the self-electophoresis mechanism of the Pt-Au rod colloidal motors.[19] (B) The chemotaxis of the Pt-Au rod colloidal motors toward the H_2O_2 source.[20] (C) The inhomogeneous distribution of the Pt-Au rod colloidal motors in different H_2O_2-concentration area. [20] Reproduced with permission.[19,20] Copyright 2010 and Copyright 2007, American Physical Society.

10.1002/chem.202202319

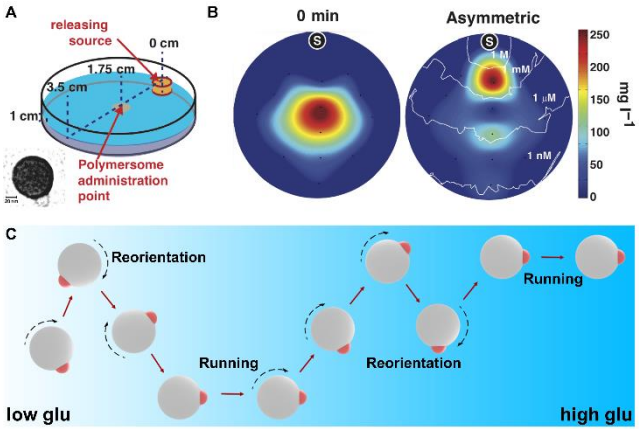

Figure 3. (A) The scheme of the chemotactic experiments of the polymersome colldoidal motors. Inset: The TEM image of the polymersome colloidal motor.[12] (B) The distribution of the polymersome colloidal motors in the glucose gradient.[12] (C) The simulated reorientation behavior of the polymersome colloidal motors in the chemotaxis. Reproduced with permission.[12] Copyright 2017, American Association for the Advancement of Science.

370 nm in diameter) which can self-propel according to the self-electrophoresis mechanism (Figure 2A).[19] It was found that the Pt-Au rodlike colloidal motors could aggregate at the H_2O_2-enriched area.[20] In the experiment, the hydrogel containing H_2O_2 was settled in the center of the chamber and then the chamber was filled with deionized water consist of Pt-Au rodlike colloidal rodlike colloidal motors. Thus, the H_2O_2 gradient could be established in the solution. As the experiment progressed, more and more Pt-Au rodlike colloidal motors aggregated at the surface of the hydrogel, as shown in Figure 2B. Furthermore, they placed four capillaries containing 0%, 0.1%, 1%, and 10% H_2O_2 respectively in the solution containing the Pt-Au rodlike colloidal motors. As shown in Figure 2C, the capillary with 10% H_2O_2 contained the highest concentration of the Pt-Au rodlike colloidal motors, 1% in the second, 0.1% in the third, and 0% in the lowest. Based on the results that Pt-Au rodlike colloidal motors aggregated in the higher-concentration of H_2O_2, the chemotactic theory was explained as the enhanced diffusion mechanism. The H_2O_2 concentration increased when the Pt-Au rodlike colloidal motors moved up the gradient, thus the reaction rate of the Pt-Au rodlike colloidal motors was also enhanced, which resulted in the higher diffusion coefficient. In this case, the Pt-Au rodlike colloidal motors realize the higher average displacement at H_2O_2-higher area. The asymmetric distribution of the displacement in the H_2O_2 gradient resulted in the net drift of the Pt-Au rodlike colloidal motors toward the H_2O_2 source. This work first demonstrated the feasibility of the chemotactic colloidal motors and explained the mechanism of the artificial chemotaxis, which provides the research direction for the chemotactic colloidal motors. However, the chemotactic mechanism was not demonstrated by directly observing the chemotactic behaviors of the colloidal motors in the experiments, which resulted in the flaws in the theory. Afterwards, Joseph *et al.* realized the chemotaxis of the submicrometer-sized colloidal motors.[12] They prepared a kind of polymersome colloidal motors with a diameter of 100 nm (inset of Figure 3A) powered by the cascade reaction of the glucose oxidase (GOx) and catalase (Cat). As shown in Figure 3A, glucose gradients were established by soaking agarose gels containing glucose immersed at the edge of the petri dish filled with PBS. Then the polymersome colloidal motors were injected in the middle of the petri dish. As the left panel shown in Figure 3B, the polymersome colloidal motors could be detected at the injection position at 0 min. After 10 min, the polymersome colloidal motors were found toward the glucose source (right panel in Figure 3B). In this work, they simulated the track trajectories of the polymersome colloidal motors in the chemotaxis and inferred that the chemotactic polymersome colloidal motors depended on the reorientation mechanism. As shown in Figure 3C, when the self-propelled direction of polymersome colloidal motors deviated from the gradient due to the strong Brownian rotational diffusion, the motors tended to reorient toward the gradient with consequently running. Thus the colloidal motor could realize positive chemotaxis. The simulation of the reorientation mechanism for the chemotaxis was consistent with the chemotactic theory predicted before.[13] As the Golestanian *et al.* described, different from other mechanisms for the directional motion, the torque-driven reorientation mechanism could be regarded as the true chemotaxis of the colloidal motors since the couple between the self-propelled motion and the substrate gradient drove the colloidal motors toward the substrate source actively.[13c] This work not only realizes the positive chemotaxis for the submicrometer-sized colloidal motors and proposes a theoretical model for the chemotaxis, but also demonstrates the potential in the biomedical field. However, the direct evidence for the torque-driven reorientation mechanism in the chemotaxis is not derived since the reorientation behavior in the chemotaxis is not observed in the experiments.

As mentioned above, the chemotaxis of both the micrometer- and submicrometer-sized colloidal motors has been realized experimentally, however, the underlying chemotactic mechanism is still unclear due to the lack of the direct experimental proof of the reorientation behavior. As reported previously, Golestanian *et*

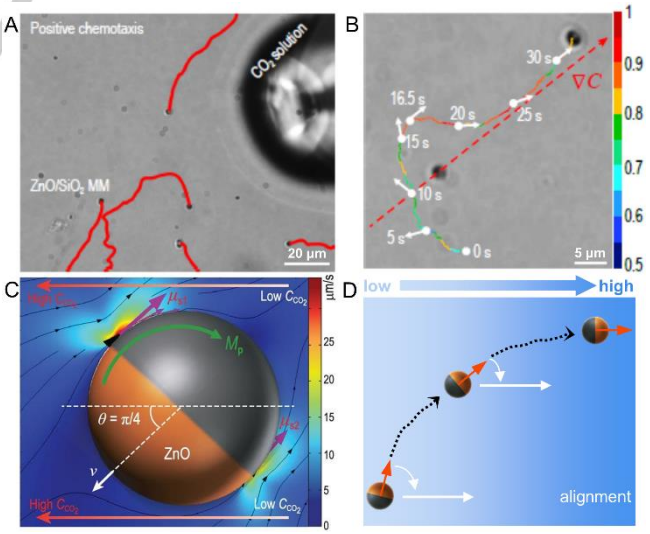

Figure 4. (A) The chemotactic process and corresponding (B) reorientation behavior and (C) fluid field of the ZnO-based Janus colloidal motors.[21] (D) The torque-driven reorientation mechanism for the ZnO-based Janus colloidal motors. Reproduced with permission.[21] Copyright 2021, Oxford University Press.

10.1002/chem.202202319

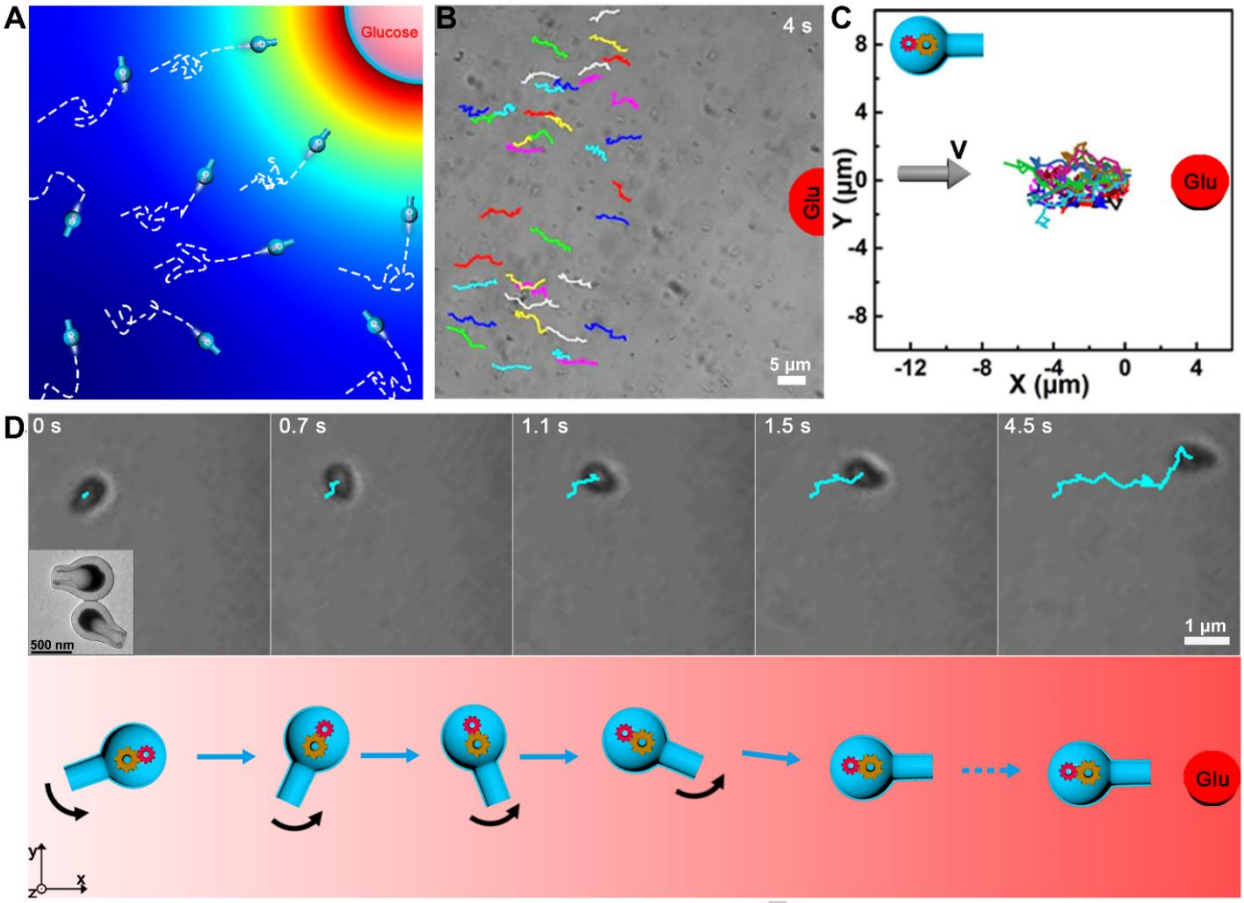

Figure 5. (A) The scheme and corresponding (B) time lapse image, (C) track trajectories and (D) reorientation behavior of the flasklike colloidal motors in the chemtaxis. Inset: The TEM image of the flasklike colloidal motors.[22] Reproduced with permission.[22] Copyright 2022, Wiley-VCH.

al. predicted that the colloidal motors can realize directional motion through four kinds of motion behaviors as reorientation, polar run-and-tumble, net drift beyond rotational diffusion and net drift at all times, in which the four kinds of behaviors corresponded different mechanisms.[13c] Thus, the direct observation of the chemotactic behaviors in the experiments plays the crucial role in the chemotactic research, which can determine the underlying chemotactic mechanism behind the colloidal motors. Guan *et al.* first reported the direct observation of the chemotactic reorientation behavior of the micrometer-sized Janus colloidal motors.[21] They prepared the ZnO-based Janus colloidal motors by coating the SiO_2 on the half of the surface of the ZnO microspheres, whose diameter was approximately 2.5 μm. In the solution with CO_2, the ZnO surface of the colloidal motors can react as:

$$ZnO + 2CO_2 + H_2O \rightarrow Zn^{2+} + 2HCO_3^- \quad (1)$$

which could drive the ZnO-based colloidal motors to move toward the ZnO side. To investigate the chemotaxis of the ZnO-based Janus colloidal motors, the CO_2 gradient was established by filling the micropipette with CO_2 solution. As shown in Figure 4A, the ZnO-based Janus colloidal motors could aggregate toward the CO_2 source. The motion behavior of the ZnO-based Janus colloidal motors was recorded by optical microscopy in the Figure 4B. When the self-propelled direction was not parallel to the gradient, the ZnO-based Janus colloidal motors tended to rotate to align the self-propelled direction parallel to the gradient. The fluid flow field in Figure 4C showed that when the self-propelled direction of ZnO-based Janus colloidal motors misaligned with the CO_2 gradient, the different reaction rates due to the asymmetric distribution of the CO_2 induced an unbalanced slip velocity across the colloidal motor, which resulted in the torque $\boldsymbol{M}_p$ to force the colloidal motor to rotate the self-propelled direction parallel to the CO_2 gradient. Therefore, the chemotaxis of the ZnO-based Janus colloidal motors is in agreement with the torque-driven reorientation mechanism as shown in Figure 4D, in which the ZnO-based Janus colloidal motors reorient the self-propelled direction toward the gradient in the chemotaxis.

Different from the micrometer-sized colloidal motors, the Brownian motion has much stronger influence on the submicrometer-sized colloidal motors. Accordingly, the motion behavior of the submicrometer-sized colloidal motors is difficult to be recorded experimentally. To address this issue, Zhou *et al.* designed the flasklike colloidal motors with 850 nm body length and 700 nm spherical bottom, which are loaded with GOx and Cat inside the cavity to realize a positive chemotaxis in a glucose gradient.[22] The flasklike colloidal motors could self-propel in the glucose solution through the enzymatic cascade reaction of GOx and Cat with the opening forward. To observe the chemotaxis of the flasklike colloidal motors, the glucose gradient was established by using a piece of agarose gel containing glucose. Once sensing the glucose gradient, the flasklike colloidal motors could exhibit a positive chemotaxis toward the glucose source as

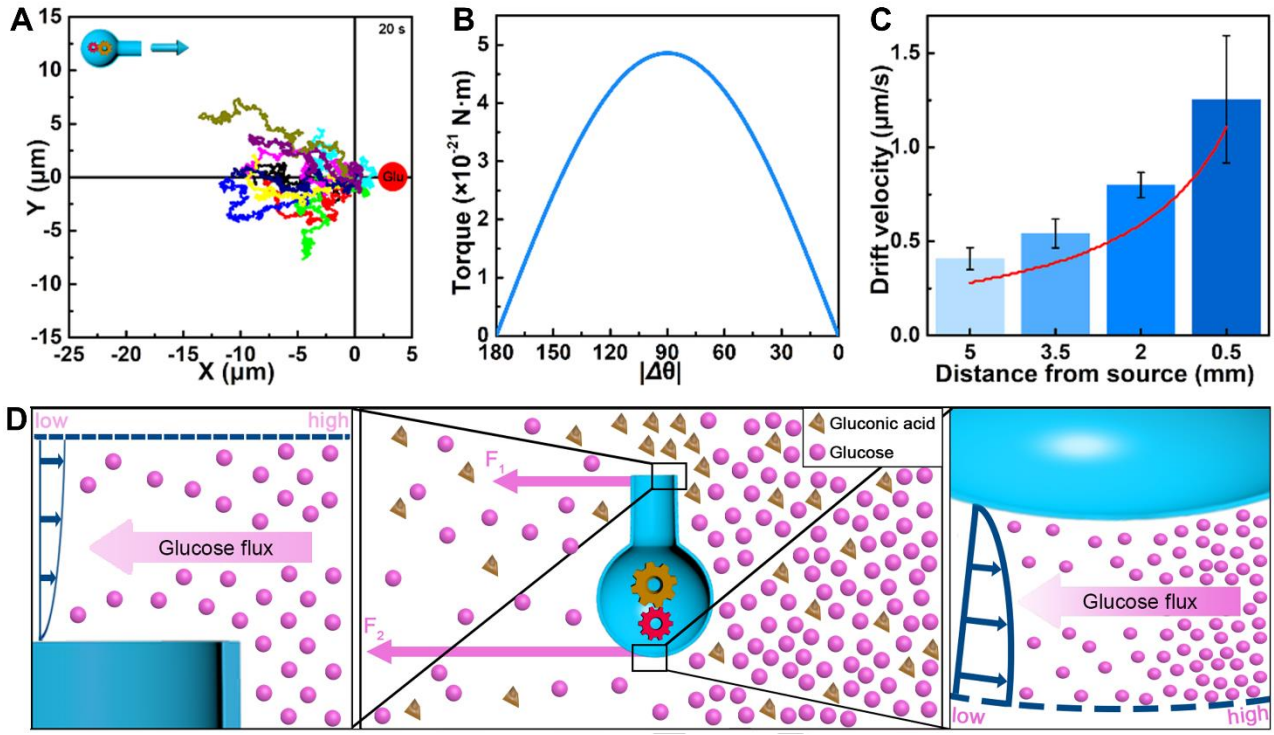

Figure 6. (A) The simulated track trajectories, (B) torque and (C) drift velocity of the flasklike colloidal motors at different distances from the source in the chemotaxis.[22] (D) The scheme of the reorientation mechanism for the flask-like colloidal motors in the chemotactic process.[22] Reproduced with permission.[22] Copyright 2022, Wiley-VCH.

shown in Figure 5A-C. Further analysis revealed that the chemotactic ability was in proportion to the glucose gradient. Due to the unique flasklike shape, the chemotactic behavior could be distinguished clearly, which is the key to the research on the chemotactic mechanism. As shown in Figure 5D, these flasklike colloidal motors could reorient the self-propelled direction parallel to the gradient, and thus could drive the colloidal motors to approach the glucose source. The reorientation behavior of the submicrometer-sized flasklike colloidal motors in the chemotaxis provides the direct evidence for torque-driven reorientation mechanism, which expands the potential of the chemotactic colloidal motors in the biomedical fields.

Torque-driven Reorientation Mechanism

Beyond the above-mentioned work on artificial chemotaxis, Zhou *et al.* further developed the chemotactic mechanism for the chemotaxis of the colloidal motors based on the chemotactic experiment of the flasklike colloidal motors.[22] First, due to the mass continuity and Fick's law, the glucose flux generated from the cylindrical agarose gel can be considered inversely proportional to the distance from the center of the source as $j \propto r^{-1}$. Thus, the glucose concentration can be established as:

$$c(r) = c_0 - c_1 \ln(r) \quad (2)$$

where c_0 and c_1 are the parameters determined by the boundary condition of the chemotactic device. The self-propelled velocity of the flasklike colloidal motors is proportional to the glucose concentration under the maximum reaction rate.[22-23] Given the relation between the glucose concentration and the distance from the center of the glucose source as shown in equation (2), the self-propelled velocity can be relative to the distance from the center of the glucose source as:

$$v_s(r) = v_0 - v_1 \ln(r) \propto c(r) \quad (3)$$

where v_0 and v_1 are the free parameters. On the other hand, as the GOx and Cat are loaded in the cavity of the flasklike colloidal motors, the catalytic reaction depends on the diffusion of the reactant glucose and the product gluconic acid through the opening. Thus, the effective glucose concentration in the glucose gradient relies on the orientation of the opening, in which the maximum and minimum self-propelled velocity correspond to the opening toward or against the glucose source. In this condition, the self-propelled velocity v_s can be described as:

$$v_s(r,\theta) = [v_0 - v_1 \ln(r)][1 + r^{-1}\delta cos\theta] \quad (4)$$

where δ is also the free parameter, θ is the orientation between the self-propelled direction and the glucose gradient. According to the chemotactic experiments, the chemotactic velocity $v_s(r,\theta)cos\theta$ which refers to the velocity projected from the self-propelled velocity to the gradient can be obtained as the function of the θ at different distances from the source. Thus, the free parameters v_0, v_1 and δ can be derived by fitting the $v_s(r,\theta)cos\theta$ vs θ curve. Furthermore, it is assumed that the reorientation of the flasklike colloidal motors originates from the torque generated by the asymmetrical self-diffusiophoretic forces across the long axis of the flasklike colloidal motors. Due to the reactive site and the diffusion of the glucose, it can be easily inferred that the glucose gradient at the opening is smaller than the bottom. Thus, the phoretic torque can reorient the self-propelled direction toward the gradient. In this condition, the torque is in proportion to the glucose gradient and relative to the orientation of the flasklike colloidal motors where the torque is maximum at $\theta = \pm\pi/2$ and

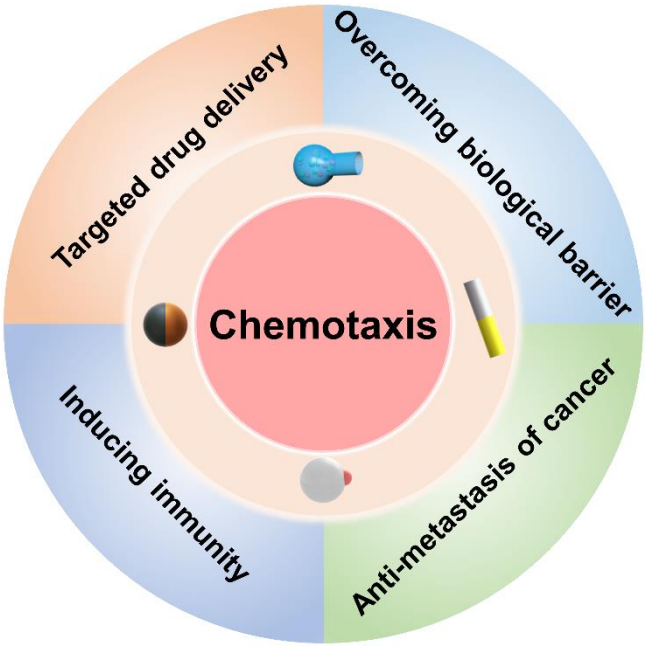

Figure 7. The potential biomedical applications of the chemotactic colloidal motors.

minimum at $\theta = 0, \pi$. Hence, the phoretic torque τ can be taken as:

$$\tau(r,\theta) = -\tau_0 r^{-1} sin\theta \quad (5)$$

where τ_0 is the fitting prefactor. As mentioned above, the phoretic torque is proportional to the glucose gradient, which is also demonstrated by the chemotactic experiments. It is found that the flasklike colloidal motor orientation θ tends to maintain less than $\pi/2$. Here, it is assumed that the flasklike colloidal motor orientation obeys an equilibrium probability distribution, and by relating the torque $\tau(r,\theta)$ to the effective angle potential $U(r,\theta) = -\tau_0 r^{-1} cos\theta$, the distribution of the flasklike colloidal motor orientation can be described as:

$$P(r,\theta) \propto \exp(\beta\tau_0 r^{-1} cos\theta) \quad (6)$$

where $\beta = 1/k_B T$, with k_B the Boltzmann constant, T the temperature. By fitting the equation (6) to the experimental data, the value of $\beta\tau_0$ can be obtained. Until now, the free parameters v_0, v_1, δ and $\beta\tau_0$ are derived from the fitting of the experimental data. In this case, the translational and rotational dynamics in the chemotaxis of the flasklike colloidal motors can be simulated through the overdamped Langevin equation as:

$$\gamma \boldsymbol{v} = \gamma v_s \boldsymbol{n} + \xi \quad (7)$$

$$\gamma_r \omega = \tau + \xi_r \quad (8)$$

where γ and γ_r are the translational and rotational friction coefficient, $\boldsymbol{v}$ is the instantaneous speed of the flasklike colloidal motor, $\boldsymbol{n}$ is unit vector of the self-propelled direction of the flasklike colloidal motor, ω is the rotational velocity of the flasklike colloidal motors. ξ and ξ_r are the Gaussian-distributed stochastic force and torque with zero mean and possessing the variance:

$$\langle \xi_\alpha(t)\xi_\beta(t')\rangle = 2k_B T\gamma\delta_{\alpha\beta}\delta(t-t') \quad (9)$$

$$\langle \xi_{r\alpha}(t)\xi_{r\beta}(t')\rangle = 2k_B T\gamma_r\delta_{\alpha\beta}\delta(t-t') \quad (10)$$

where α and β are the Cartesian components. Substituting the parameters v_0, v_1, δ and $\beta\tau_0$ into equation (7) and (8), thus the chemotactic track trajectories can be obtained as shown in Figure 6A. The track trajectories show the positive chemotaxis toward the glucose, which is consistent with the experimental data as shown in Figure 5C. The result proves the correctness of the chemotactic theory.

Since the chemotaxis can be described by the overdamped Langevin equation, the dynamics of the chemotactic process can be further derived. Firstly, combing the equation (5) and the mean torque balance condition,

$$\gamma_r \omega = \tau \quad (11)$$

the relation between the orientational angle θ and evolution time t can be derived as:

$$t = \omega_0^{-1} \ln[(csc\theta - cot\theta)/(csc\theta_0 - cot\theta_0)] \quad (12)$$

According to equation (12), the phoretic torque can be derived, which is shown in Figure 6B. It can be found that during the reorientation process, the torque will increase when the orientational angle θ deviates 0 or π, and the torque will be the largest when $\theta = \pi/2$. The torque can drive the self-propelled direction of the flasklike colloidal motors parallel to the gradient, which can also maintain the orientation. The reorientation process has a positive effect on the chemotaxis. Furthermore, the r-dependence drift velocity in the xy-plane is dependent on the orientation of the flasklike colloidal motors, which can be derived based on equation (4) and (6) as:

$$v_d = \int_0^{2\pi} P(r,\theta)\, v_s(r,\theta) cos\theta d\theta \quad (13)$$

which can fit the drift velocity in the experimental data well as shown in Figure 6C.

According to the overdamped Langevin equation, the chemotaxis of the flasklike colloidal motors is successfully modeled as shown in Figure 6D. Taking the flasklike colloidal motor's axis perpendicular to the gradient as example. As reported previously[23], the phoretic force for the hydrophilic flasklike colloidal motors suffered from the glucose gradient is higher than that of gluconic acid gradient. Thus, the major propulsion force can be considered originating from the glucose gradient, which can be described as follows:

$$F = \mu\alpha\partial c \quad (14)$$

where F is the phoretic force, μ is the mobility of the flasklike colloidal motors, α is the diffusiophoretic factor, and ∂c is the local concentration gradient of the glucose. Since the material and solute are the same, μ and α are the same for the opening and bottom. Here, the value of $\mu\alpha$ is negative for the hydrophilic colloidal motors, which causes the direction of the F anti-parallel to the ∂c. In this case, when the flasklike colloidal motor is perpendicular to the gradient, the phoretic force at the opening and the bottom can be described by the equation (14) as follows:

$$F_1 = \mu\alpha\partial c_1 \quad (15)$$

$$F_2 = \mu\alpha\partial c_2 \quad (16)$$

where F_1 and F_2 are the phoretic force generated at the opening and bottom respectively. As the reaction occurs, the glucose at the opening will be consumed so that the glucose gradient at the opening would be diluted because of the glucose consumption by the catalytic reaction, which leads to the result of $\partial c_1 < \partial c_2$, and thus $|F_1| < |F_2|$ with the same direction as shown in Figure 6D. Due to the asymmetric force distribution of the phoretic force, the opening of the flasklike colloidal motors can rotate to face the glucose source. As the flasklike colloidal motors self-propelled with opening forward and combining the self-propelled motion and the reorientation, the flasklike colloidal motors can perform a positively chemotactic motion. This study not only provides the direct evidences for the torque-driven reorientation mechanism of the submicrometer-sized colloidal motors, but also proposes an excellent physical model to explain the underlying chemotactic mechanism of the submicrometer-sized colloidal motors.

Conclusion and Future Perspectives

We have reviewed the experimental and theoretical researches of the chemotactic colloidal motors on the micrometer-sized and submicrometer-sized scales. The experimental verification of chemotactic colloidal motors, especially the submicrometer-sized colloidal motors, not only demonstrates the torque-driven reorientation mechanism, but also meet the requirement of the biomedical applications such as precise medicine and active targeting. With the excellent property of precise motion control, it can be expected that the chemotactic colloidal motors can have great application potential in the biomedical field as shown in Figure 7. With the exist of the biological barrier such as the BBB, drugs would be prevented outside the diseased site. In this case, owing to the small size and active directional motion, the submicrometer-scale chemotactic colloidal motors can cross the biological barrier and self-navigate toward the lesion area.[11a, 12] Furthermore, as the cancer has the interstitial pressure, which prevents the diffusion of the drug and oxygen carriers toward the deep site of the cancer tumor, so that the cancer can be not easily healed. In this condition, the chemotactic colloidal motors can penetrate deeply in tumor. Combining relative catalysts such as the catalase, the oxygen can be supplied to the deep tumor region to further prevent tumor metastasis.[11b] Beyond the drug delivery, researchers have found drug-free treatments that rely on chemotactic colloidal motors. In this method, the colloidal motors were modified with specific chemicals to simulate the "eat me" signal to macrophages when the colloidal motors chemotaxis to the lesion site, so that the diseased cells can be cleared by the immune system.[24] Although it has been made great progress in the chemotactic mechanism, there are also challenges and limitation for the chemotactic colloidal motors toward the biomedical applications. First, the chemotaxis has been verified in the individuals of colloidal motors, however, the chemotactic behaviors of the colloidal motor swarms is not clear yet. It is necessary to fully understand the chemotactic mechanism of the colloidal motor swarms in complex environments for the design of intelligent colloidal motors for active drug delivery in practice. More particularly, given that the *in vivo* complex environment, the realization of the chemotaxis-based self-navigation of the colloidal motors is difficult due to the biological barriers such as immune clearance, blood flow, blood network, cell membrane, collective motion. Overcoming these challenges to perform the chemotaxis *in vivo* would be the key goal of the chemotactic colloidal motors in the biomedical field.

Acknowledgements

This work is financially supported by the National Natural Science Foundation of China (Nos. 22193033, 22172044 and 11874397), the start-up grant of Wenzhou Institute, University of Chinese Academy of Sciences (WIUCASQD2021044), and the State Key Laboratory of Robotics at the Shenyang Institute of Automation, Chinese Academy of Sciences (Grant no. 2019-O02).

Conflict of interest

The authors declare no conflict of interest.

Keywords: colloidal motor • self-propulsion • chemotaxis • reorientation • diffusiophoresis

[1] a) J. R. Howse, R. A. L. Jones, A. J. Ryan, T. Gough, R. Vafabakhsh and R. Golestanian, *Phys. Rev. Lett.* **2007**, *99*, 048102; b) T. Patiño, X. Arqué, R. Mestre, L. Palacios and S. Sánchez, *Acc. Chem. Res.* **2018**, *51*, 2662-2671; c) Z. Xiao, S. Duan, P. Xu, J. Cui, H. Zhang and W. Wang, *ACS Nano* **2020**, *14*, 8658-8667.

[2] a) J. Jiang, Z. Yang, A. Ferreira and L. Zhang, *Adv. Intell. Syst.* **2022**, *4*, 2100279; b) J. Mujtaba, J. Liu, K. K. Dey, T. Li, R. Chakraborty, K. Xu, D. Makarov, R. A. Barmin, D. A. Gorin, V. P. Tolstoy, G. Huang, A. A. Solovev and Y. Mei, *Adv. Mater.* **2021**, *33*, 2007465; c) S. Tang, F. Zhang, H. Gong, F. Wei, J. Zhuang, E. Karshalev, B. Esteban-Fernández de Ávila, C. Huang, Z. Zhou, Z. Li, L. Yin, H. Dong, R. H. Fang, X. Zhang, L. Zhang and J. Wang, *Sci. Rob.* **2020**, *5*, eaba6137; d) D. Xu, J. Hu, X. Pan, S. Sánchez, X. Yan and X. Ma, *ACS Nano* **2021**, *15*, 11543-11554.

[3] R. Colin, K. Drescher and V. Sourjik, *Nat. Commun.* **2019**, *10*, 5329.

[4] C. Chen, X. Chang, P. Angsantikul, J. Li, B. Esteban-Fernández de Ávila, E. Karshalev, W. Liu, F. Mou, S. He, R. Castillo, Y. Liang, J. Guan, L. Zhang and J. Wang, *Adv. Biosyst.* **2018**, *2*, 1700160.

[5] D. A. Bloes, D. Kretschmer and A. Peschel, *Nat. Rev. Microbiol.* **2015**, *13*, 95-104.

[6] C. H. Y. Wong, B. Heit and P. Kubes, *Cardiovasc. Res.* **2010**, *86*, 183-191.

[7] J. Y. Kim, X. Xin, E. K. Moioli, J. Chung, C. H. Lee, M. Chen, S. Y. Fu, P. D. Koch and J. J. Mao, *Tissue Eng., Part A* **2010**, *16*, 3023-3031.

[8] L. Wang, Y. Li, Y. Liu, L. Zuo, Y. Li, S. Wu and R. Huang, *Fish Shellfish Immunol.* **2019**, *87*, 721-729.

[9] a) Y. Ye, F. Tong, S. Wang, J. Jiang, J. Gao, L. Liu, K. Liu, F. Wang, Z. Wang, J. Ou, B. Chen, D. A. Wilson, Y. Tu and F. Peng, *Nano Lett.* **2021**, *21*, 8086-8094; b) M. Mathesh, J. Sun, F. van der Sandt and D. A. Wilson, *Nanoscale* **2020**, *12*, 22495-22501; c) M. Guix, A. K. Meyer, B. Koch and O. G. Schmidt, *Sci. Rep.* **2016**, *6*, 21701.

[10] a) M. You, C. Chen, L. Xu, F. Mou and J. Guan, *Acc. Chem. Res.* **2018**, *51*, 3006-3014; b) W. Xu, H. Qin, H. Tian, L. Liu, J. Gao, F. Peng and Y. Tu, *Appl. Mater. Today* **2022**, *27*, 101482.

[11] a) H. Zhang, Z. Cao, Q. Zhang, J. Xu, S. L. J. Yun, K. Liang and Z. Gu, *Small* **2020**, *16*, 2002732; b) W. Yu, R. Lin, X. He, X. Yang, H. Zhang, C. Hu, R. Liu, Y. Huang, Y. Qin and H. Gao, *Acta Pharm. Sin. B* **2021**, *11*, 2924-2936.

[12] A. Joseph, C. Contini, D. Cecchin, S. Nyberg, L. Ruiz-Perez, J. Gaitzsch, G. Fullstone, X. Tian, J. Azizi, J. Preston, G. Volpe and G. Battaglia, *Sci. Adv.* **2017**, *3*, e1700362.

[13] a) M. N. Popescu, W. E. Uspal, C. Bechinger and P. Fischer, *Nano Lett.* **2018**, *18*, 5345-5349; b) T. Bickel, G. Zecua and A. Würger, *Phys. Rev. E* **2014**, *89*, 050303; c) S. Saha, R. Golestanian and S. Ramaswamy, *Phys. Rev. E* **2014**, *89*, 062316.

[14] a) C. Gao, Y. Wang, Z. Ye, Z. Lin, X. Ma and Q. He, *Adv. Mater.* **2021**, *33*, 2000512; b) J. Shao, S. Cao, D. S. Williams, L. K. E. A. Abdelmohsen and J. C. M. van Hest, *Angew. Chem., Int. Ed.* **2020**, *59*, 16918-16925; c) W. Wang and C. Zhou, *Adv. Healthcare Mater.* **2021**, *10*, 2001236; d) M. Wan, T. Li, H. Chen, C. Mao and J. Shen, *Angew. Chem., Int. Ed.* **2021**, *60*, 13158-13176; e) Z. Wu, Y. Chen, D. Mukasa, O. S. Pak and W. Gao, *Chem. Soc. Rev.* **2020**, *49*, 8088-8112.

[15] M. Wan, H. Chen, Q. Wang, Q. Niu, P. Xu, Y. Yu, T. Zhu, C. Mao and J. Shen, *Nat. Commun.* **2019**, *10*, 966.

[16] J. W. Jolles, N. J. Boogert, V. H. Sridhar, I. D. Couzin and A. Manica, *Curr. Biol.* **2017**, *27*, 2862-2868.e2867.

[17] V. Sourjik and N. S. Wingreen, *Curr. Opin. Cell Biol.* **2012**, *24*, 262-268.

[18] S. Bi and V. Sourjik, *Curr. Opin. Microbiol.* **2018**, *45*, 22-29.

[19] J. L. Moran, P. M. Wheat and J. D. Posner, *Phys. Rev. E* **2010**, *81*, 065302.

[20] Y. Hong, N. M. K. Blackman, N. D. Kopp, A. Sen and D. Velegol, *Phys. Rev. Lett.* **2007**, *99*, 178103.

[21] F. Mou, Q. Xie, J. Liu, S. Che, L. Bahmane, M. You and J. Guan, *Natl. Sci. Rev.* **2021**, *8*, nwab066.

[22] C. Zhou, C. Gao, Y. Wu, T. Si, M. Yang and Q. He, *Angew. Chem., Int. Ed.* **2022**, *61*, e202116013.

[23] C. Gao, C. Zhou, Z. Lin, M. Yang and Q. He, *ACS Nano* **2019**, *13*, 12758-12766.
[24] Z. Wu, M. Zhou, X. Tang, J. Zeng, Y. Li, Y. Sun, J. Huang, L. Chen, M. Wan and C. Mao, *ACS Nano* **2022**, *16*, 3808-3820.

10.1002/chem.202202319

WILEY-VCH

CONCEPT

Entry for the Table of Contents

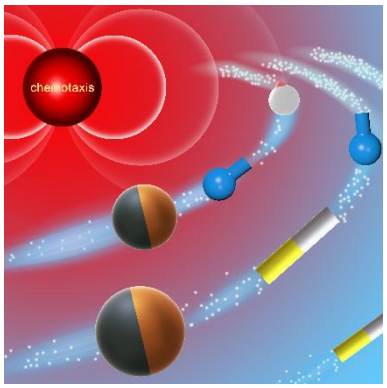

The chemotactic colloidal motors can be served as excellent physical models of non-equilibrium complex systems and also have potential in active target delivery and other biomedical applications. In this concept, both the recent experimental progress and theoretical opinion of chemotactic motors based on the torque-driven self-reorientation and alignment mechanism are discussed.

.